Current Optics and Photonics
Vol. 1, No. 4, August 2017, pp. 389-395

ISSN: 2508-7266(Print) / ISSN: 2508-7274(Online)
DOI: https://doi.org/10.3807/COPP.2017.1.4.389

Red-emitting α-$SrO{\cdot}3B_2O_3$:Sm^{2+} Phosphor for WLED Lamps: Novel Lighting Properties with Two-layer Remote Phosphor Package

Phu Tran Tin[1], Nhan K. H. Nguyen[2]*, Minh Q. H. Tran[2], and Hsiao-Yi Lee[3]

[1]*Faculty of Electronics Technology, Industrial University of Ho Chi Minh City, Ho Chi Minh City, Vietnam*
[2]*Faculty of Electrical and Electronics Engineering, Ton Duc Thang University, No. 19 Nguyen Huu Tho, District 7, Ho Chi Minh City, Vietnam*
[3]*Department of Electrical Engineering, National Kaohsiung University of Applied Sciences, Kaohsiung City, Taiwan*

(Received January 22, 2017 : revised June 16, 2017 : accepted June 28, 2017)

This paper investigates a method to improve the lighting performance of white light-emitting diodes (WLEDs), which are packaged using two separate remote phosphor layers, a yellow-emitting YAG:Ce phosphor layer and a red-emitting α-$SrO{\cdot}3B_2O_3$:Sm^{2+} phosphor layer. The thicknesses of these two layers are 800 μm and 200 μm, respectively. Both of them are examined in conditions where the average correlated color temperatures (CCT) are 7700 K and 8500 K. For this two-layer model, the concentration of red phosphor is varied from 2% to 30% in the upper layer, while in the lower layer the yellow phosphor concentration is kept at 15%. It was found interestingly that the lighting properties such as color rendering index (CRI) and luminous flux are enhanced significantly, while the color uniformity is maintained in a relatively close range to the one of one-layer configuration (measured at the same correlated color temperature). Besides, the transmitted and reflected light of each phosphor layer are revised by combining Kubelka-Munk and Mie-Lorenz theories. Through analysis, it is demonstrated that the packaging configuration of two-layer remote phosphor that employs red-emitting α-$SrO{\cdot}3B_2O_3$:Sm^{2+} phosphor particles provides a practical solution for general WLEDs lighting.

Keywords : Remote phosphor structure, Two-layer package, Luminous flux, Color rendering index, Light emitting diodes (LEDs)
OCIS codes : (230.3670) Light-emitting diodes; (260.3800) Luminescence; (330.1710) Color measurement

I. INTRODUCTION

White light-emitting diodes (WLEDs) that possess high luminous and energy efficiency, small volume, and green environment are good substitutions for conventional incandescent and fluorescent lamps [1]. However, improvements are still needed in light extraction and thermal conduction from the WLEDs packages [2, 3]. Blue or UV LEDs combined with phosphor materials can emit white light by converting the generated radiation to the complementary color. In general lighting applications, the phosphor-converted LEDs need to have a broadband spectrum which covers the visible region to achieve high color rendering index (CRI). Otherwise, a multilayer phosphor package with different emitting spectra should be selectable. However, due to the electron trapping phenomenon and the inelastic scattering between phosphor materials in the LED package, more emission power of the LED is lost as the phosphor concentration increases [4]. Phosphor arrangement and geometry can have a significant role in enhancing energy efficiency and reducing light trapping in the LED package. Novel phosphor configurations, e.g. scattered photon extraction (SPE) package [5], remote phosphor with a hemispherical dome [6, 7], as well as the method to enhance light extraction by using commercial YAG:Ce^{3+} (yellow) and SrS:Eu^{2+}, $Sr_2Si_5N_8$:Eu^{2+} (red) phosphorus [9, 10] have been

*Corresponding author: nguyenhuukhanhnhan@tdt.edu.vn
Color versions of one or more of the figures in this paper are available online.

suggested and confirmed by ray-tracing analysis and experiments. Recently, some researchers have also recommended that a low-concentration phosphor mixture could provide improvement in the output luminous flux and the shift of color coordinates [11]. Other authors proposed an approach to enhance color homogeneity by adding SiO_2 [12] or using Y_2O_3:Eu^{3+} [8]. Another method to improve color quality is mixing a red phosphor like SrS:Eu^{2+} with a yellow or green phosphor, like YAG:Ce^{3+} or $SrGa_2S_4$:Eu^{2+} [13]. These studies are groundwork for the concept of reducing the backscattering light to an LED chip and improving the phosphor converted efficiency [14]. Single-layer, bi-layer or multi-layer structures with a different phosphor concentration at each layer have been reported in [15, 16].

This paper deploys a two-layer remote phosphor structure using a α-$SrO{\cdot}3B_2O_3$:Sm^{2+} red phosphor layer above a YAG:Ce yellow phosphor layer, and investigates the variance of CRI, CCT deviation and luminous flux that can be caused by adjusting the concentration of red emitting α-$SrO{\cdot}3B_2O_3$:Sm^{2+} phosphor. The characteristics of the proposed model are compared to a one-layer remote phosphor WLED (RP-WLED) package, which has been implemented in a previous study [18]. This investigation can be separated into two tasks: 1) analyzing the effect of α-$SrO{\cdot}3B_2O_3$:Sm^{2+} concentration on the lighting performance of two-layer RP-WLED by combining Kubelka-Munk and Mie-Lorenz theories; 2) using the LightTools software to simulate the physical models of one-layer and two-layer RP-WLED.

Red-emitting α-$SrO{\cdot}3B_2O_3$:Sm^{2+} phosphor, which has a peak wavelength of 680 nm, is a red polycrystalline phosphor. It is synthesized by three oxides including strontium oxide (SrO), samarium oxide Sm_2O_3, and orthoboric acid (H_3BO_3). Sm^{2+} ion is added to the polycrystalline phosphor for enhancing its absorbability at excitation spectrum region from 420 nm to 502 nm, which results in higher luminous efficiency [17]. Besides, with the advantage of excellent thermal and chemical stability, α-$SrO{\cdot}3B_2O_3$:Sm^{2+} can be employed for compensating red light, and hence, increasing the color quality of LED lamps. However, until now, there has been no study that employs α-$SrO{\cdot}3B_2O_3$:Sm^{2+} for two-layer RP-WLEDs.

II. CONSTRUCTION AND ANALYSIS OF PHYSICAL MODEL

The LightTools and SolidWorks are necessary to build the remote phosphor multi-chip WLEDs model, which is shown in Fig. 1. The RP-WLED reflector has a bottom length of 8 mm, a height of 2.07 mm and a length of 9.85 mm at its top surface. The one-layer remote phosphor configuration, which has a fixed thickness d = 1 mm, is mixed by α-$SrO{\cdot}3B_2O_3$:Sm^{2+} red phosphor and YAG:Ce yellow phosphor and it is 0.8 mm far from the 9 LED chips as shown in Fig. 1(a). Each chip with a square base of 1.14 mm^2 and a height of 0.15 mm is bounded in the cavity of the reflector. The radiant flux of each blue chip is 1.16 W at wavelength 455 nm. Fig. 1(b) shows two-layer configuration with α-$SrO{\cdot}3B_2O_3$:Sm^{2+} red phosphor layer having fixed thickness of 0.2 mm and YAG:Ce yellow phosphor layer having fixed thickness of 0.8 mm. In order to achieve light output and to investigate the effect of α-$SrO{\cdot}3B_2O_3$:Sm^{2+} with the same CCT for both types of the studied RP-WLED packages, the amount of red-emitting phosphor-silicone mixture is adjusted while the concentration of yellow-emitting phosphor-silicone mixture is fixed at 15%. Also, the height of encapsulation is kept approximately the same in both configurations. Fig. 1(c) illustrates the package model and its real sample.

The two-flux model of Kubelka and Munk [19] is applied for two-layered structure in the analysis of light properties since it is simple and frequently yields fairly accurate results. We consider two fluxes across the x-direction through a thin layer of thickness x in YAG:Ce yellow phosphor layer of total thickness d as shown in Fig. 1(b).

The flux $I_+(x)$ in the positive x-direction is decreased by absorption and backscattering inside the layer and is increased by backscattering of the intensity $I_-(x)$ in the negative x-direction:

$$dI_+(x) = -(K+S)I_+(x)dx + SI_-(x)d \tag{1}$$

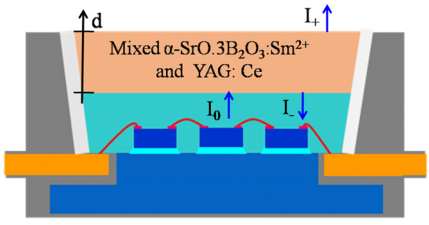

(a)

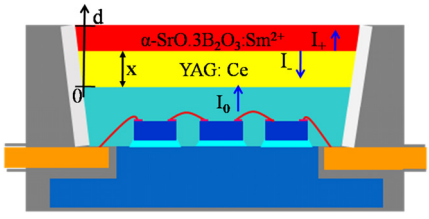

(b)

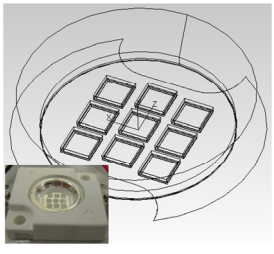

(c)

FIG. 1. Cross-sectional schematic of the RP-MWLED package: (a) mixed yellow and red phosphor structure; (b) two-layer yellow/red phosphor structure; (c) package model and its real sample.

In contrast, the flux $I_-(x)$ in the negative x-direction is decreased by absorption and backscattering inside the layer and is increased by backscattering of the intensity $I_+(x)$ in the positive x-direction:

$$dI_-(x) = (K+S)I_-(x)dx - SI_+(x)dx \tag{2}$$

The above differential equations can be solved only for the ratio $I_-(x)/\ I_+(x)$. The results for $x=0$ and $x=d$ are of special interests. The ratio $I_-(x=0)/\ I_+(x=0)$ at $x=0$ defines the diffuse reflectance R_{KM} of the two-layered structure:

$$R_{KM} = \frac{(1+\gamma)(1-\gamma)[\exp(\beta d) - \exp(-\beta d)]}{(1+\gamma)^2\exp(\beta d) - (1-\gamma)^2\exp(-\beta d)} \tag{3}$$

Analogously, the ratio $I_-(x=d)/\ I_+(x=d)$ at $x=d$ can be used to define the diffuse transmittance T_{KM} of this structure:

$$T_{KM} = \frac{4\gamma}{(1+\gamma)^2\exp(\beta d) - (1-\gamma)^2\exp(-\beta d)} \tag{4}$$

where $\gamma = \sqrt{\frac{K}{K+2S}}$ and $\beta = \sqrt{K(K+2S)}$. The quantities K and S are related to the cross-sections for extinction and scattering, C_{ext} and C_{sca}, the asymmetry parameter g which presents the amount of back and forward scattered light, and the volume density V_d of phosphor particles [20-22]:

$$K = \frac{C_{ext} - C_{sca}}{V_d} = \frac{C_{abs}}{V_d} \tag{5}$$

$$S = \frac{3}{4}\frac{C_{sca}(1-g)}{V_d} = \frac{3}{4}\frac{\delta_{sca}}{V_d} \tag{6}$$

According to Mie-Lorenz theory [23], δ_{sca} is the reduced scattering coefficient. The extinction efficiency C_{ext}, the scattering efficiency C_{sca}, and the absorption efficiency C_{abs} are normally calculated by the following equations:

$$C_{ext} = \frac{2p}{k^2}\sum_0^{\infty}(2n+1)\,\mathrm{Re}(a_n + b_n) \tag{7}$$

$$C_{sca} = \frac{2p}{k^2}\sum_0^{\infty}(2n+1)(|a_n|^2 + |b_n|^2) \tag{8}$$

where k is the wave number ($2\pi/\lambda$), and a_n and b_n are the extension factors with even and odd symmetry, respectively, which are calculated by

$$a_n(z,m) = \frac{\psi_n'(mz)\psi_n(z) - m\psi_n(mz)\psi_n'(z)}{\psi_n'(mz)\xi_n(z) - m\psi_n(mz)\xi_n'(z)} \tag{9}$$

$$b_n(z,m) = \frac{m\psi_n'(mz)\psi_n(z) - \psi_n(mz)\psi_n'(z)}{m\psi_n'(mz)\xi_n(z) - \psi_n(mz)\xi_n'(z)}, \tag{10}$$

where $\psi_n(z)$ and $\xi_n(z)$ are the Riccati - Bessel functions, z is relative to the size, which is calculated by Eq. (11), m is the refractive index of the particle which contains both the real and virtual term and depends on the ambient medium. In the WLEDs packaging, the ambient medium of phosphor particles is silicone glue. Thus the complex refractive index of a phosphor particle is calculated by $m = n_{phos}\ /\ n_{sil}$;

$$z = k.r.n_{sil} = \frac{2\pi n_{sil}}{\lambda}.r \tag{11}$$

where r is the equivalent spherical radius of phosphor particles, λ is the wavelength. n_{phos} and n_{sil} are the refractive indexes of phosphor and silicone gel, respectively.

For a two-layer structure, the transmission and reflection intensities of blue light and yellow light are most concerned, because the changes in diffuse reflectance R_{KM} and transmittance T_{KM} also result in changes in the optical properties of WLEDs. In Figs. 2 and 3, we can observe the interaction among the light scattering, reduced scattering, backscattering, and conversion inside two phosphor layers. These results are obtained by applying the above theoretical calculations with the variation of α-SrO·3B_2O_3:Sm^{2+} concentration from 2% to 35%, whereas YAG:Ce yellow phosphor concentration is chosen as 15%. The average radius of two types of phosphor configurations are set to 7.25 μm. The refractive indexes of silicone glue, α-SrO·3B_2O_3:Sm^{2+} and YAG:Ce particles are set to 1.5, 1.93, and 1.83, respectively [12].

In Fig. 2(a), it can be seen that the scattering and reduced scattering coefficients have a rapid rising trend for blue light (λ = 455 nm), yellow light (λ = 595 nm) and red light (λ = 680 nm). Moreover, scattering coefficient and reduced scattering coefficient of blue light increase higher than both yellow and red light in the yellow phosphor layer. Meanwhile, the scattering coefficient of blue light in the red phosphor layer also gets greater than for yellow light, but the reduced scattering coefficient is not much different (Fig. 2(b)). The backscattering coefficient at a wavelength of 455 nm is much larger than at the wavelength of 595 nm and 680 nm in yellow phosphor layer as shown in Fig. 3. For both blue and yellow lights in the red-emitting phosphor layer, the backscattering coefficient is much lower than the one of 680nm (red) light. These phenomena may be due to the following reasons: 1) when α-SrO·3B_2O_3:Sm^{2+} concentration rises, more blue, yellow and red light are absorbed and scattered. It becomes harder for blue and yellow light to penetrate the phosphor layer. Thus the light intensity changes extraordinarily, which implies a continuous variability of transmitted and reflected light in Fig. 4. 2) With the increasing of α-SrO·3B_2O_3:Sm^{2+} concentration, blue light is further backscattered to all

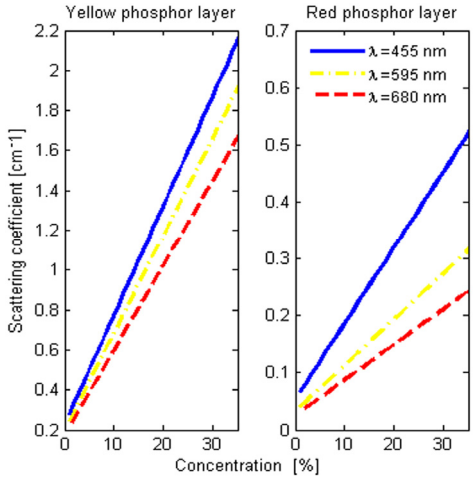

(a)

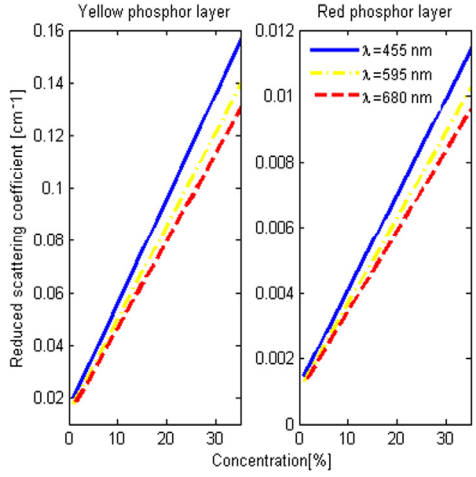

(b)

FIG. 2. The impacts of α-SrO·3B_2O_3:Sm^{2+} concentration in two-layer red/yellow phosphor structure to wavelengths 455 nm, 595 nm and 680 nm: (a) Scattering coefficient; (b) Reduced scattering coefficient.

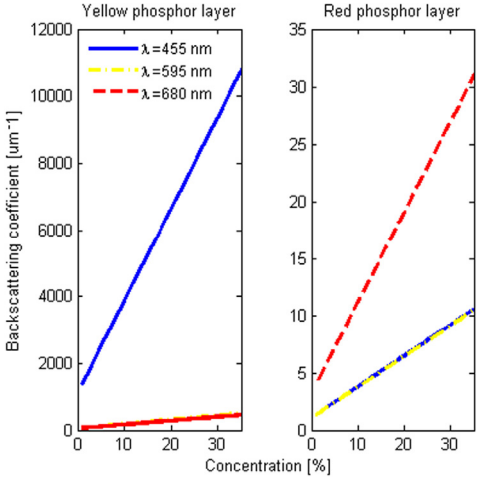

FIG. 3. Backscattering coefficient of two-layer phosphor structure to wavelengths 455 nm, 595 nm and 680 nm.

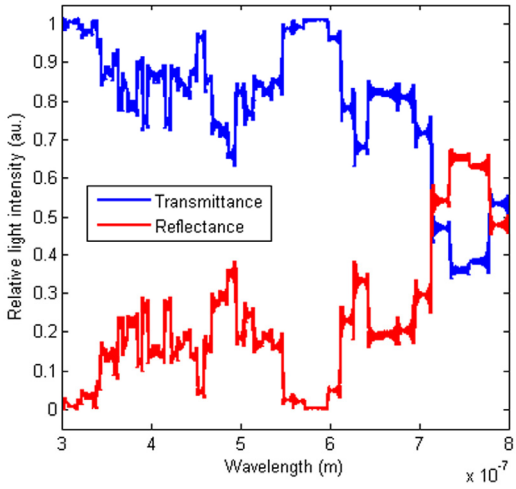

FIG. 4. Computed diffuse reflectance and transmittance spectra of two-layer phosphor structure.

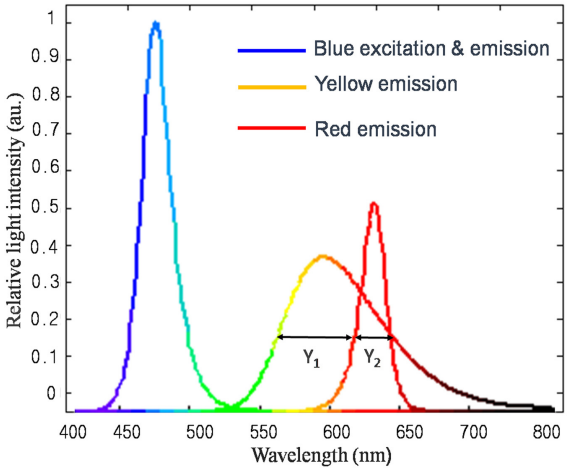

(a)

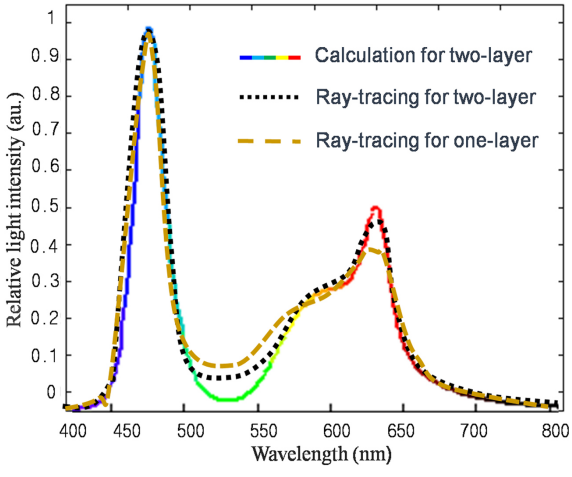

(b)

FIG. 5. (a) Emission spectra of the blue, yellow and red phosphors with the blue LED excitation light source. (b) Light distribution spectra of the theoretical calculation vs. the optical ray-tracing in the remote phosphor package at 8500 K.

directions in both yellow and red phosphor layers. Thus the reflected blue light tends to increase. The further increasing of α-SrO·3B_2O_3:Sm^{2+} concentration does not account for the rising of intensity at the incident surface, so the transmitted light intensity tends to decrease in Fig. 4. 3) When red phosphor concentration increases, at first more yellow light is converted. When concentration increases further, the effect of yellow light absorption and back-scattering is the same as blue light, which explains for the increasing in transmitted light intensity in wavelength 595 nm (shown in Fig. 4). This increase leads to a trend of wider emitted spectrum at the wavelength approximate to 595 nm, similar to the theoretical calculation spectra for two-layer LED in Fig. 5, or the changes in diffuse refl ectance and transmittance also result in the color index variation of the WLEDs.

III. RESULTS AND DISCUSSION

The emission spectra of two-layer and mixed one-layer WLED are obtained by running optical ray-tracing of LightTools™ software at the same correlated color temperature (CCT) 8500 K. With the same concentrations of yellow and red phosphor particles, the experimental results are compared to the theoretical values by using Matlab software, as shown in Fig. 5. The emission spectra of the blue, yellow and red phosphors with the blue LED excitation light source are illustrated in Fig. 5(a). These spectral power distributions are measured using the optical simulation. Both YAG:Ce and α-SrO·3B_2O_3:Sm^{2+} phosphors are simulated based on the extended Gaussian model [25] described by (13). For multiple phosphor layers (yellow and red), converted yellow radiant power from the first layer is divided into Y_1 and Y_2. While Y_1 could be absorbed by the red phosphor because it lies within the absorption (extinction - C_{ext}) spectral range of red phosphor, Y_2 cannot be absorbed by the red phosphor (Fig. 5(a)). The reflected and transmitted light would include some portion of the blue, red, and yellow (Y_1 and Y_2) radiations for blue radiant power incident on multiple phosphor layers. Therefore, the total spectral power distribution modeling for two-layer-coated phosphors white LED can be expressed as a tricolor spectrum (B-Y-R) (Fig. 5(b)).

The optical ray-tracing results matched well to the theoretical calculations in the two-layer structure. The spectral energy distributions in the WLEDs emission light and color features, in this case, are determined by the constitution of the relative luminous energy of the converted photons in phosphor layers. The reason for the disagreement in one-layer LED structure, a considerable percentage of the translated photons involved in backscattering are absorbed (*flux* $I_-(x)$) by the multichip LED. However, in the two-layer structure, these backscattering photons are taken out of the LED package, in addition to the total energy spectrum. Furthermore, the forward-emitted (*flux* $I_+(x)$) intensity from

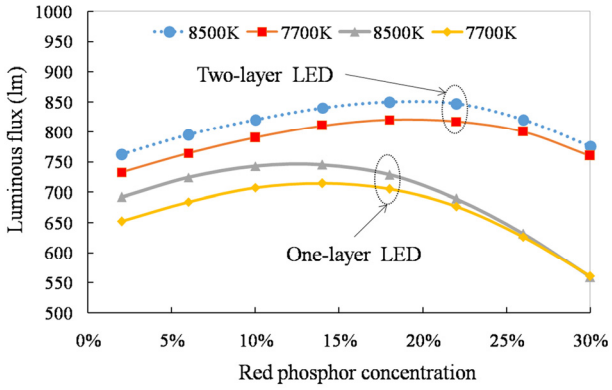

FIG. 6. Luminous flux of two-layer and mixed one-layer LEDs with various red phosphor concentrations.

the first (YAG:Ce) layer will go through the second (α-SrO·3B_2O_3:Sm^{2+}) phosphor layer and experience great scattering changes (Fig. 2(b)), while the second phosphor layer can absorb significant photon quality which drops in the excited energy band. However, the two-layer configuration attributes a higher percentage of photons to the total light energy than a single phosphor layer. For that reason, the first phosphor layer turns into the forceful layer. This leads to the result that the output luminous flux of two-layer LED is at least 17% higher than that of mixed one-layer LED. It has been demonstrated that high-concentration of red phosphor α-SrO·3B_2O_3:Sm^{2+} that exceeds 20% had disadvantages in output luminous flux as Fig. 6, due to the light scattering and absorption between phosphors' materials as mentioned above.

The inelastic scattering of light reduces the efficiency since the increased light path length leads to higher possibility of re-absorption of the incident and emitted light. Light path randomization also increases the probability of light incident on high loss areas. Compared to the mixed one-layer LED at the same CCT 7700 K and 8500 K, the increased radiation flux of blue, yellow and red components in two-layer LED indicate the decreased scattering of light inside the package. To provide further proof that the total emission power (T_{RP}), including transmittance and reflectance, can be described in the spectral formula depending on wavelength (λ) and phosphor particles radius (r), from Eq. (3) to Eq. (11) as

$$T_{RP}(\lambda) = T_{KM}(\lambda) + R_{KM}(\lambda) \tag{12}$$

From Eq. (12), the luminous flux (lumen) can be calculated from [24]

$$\Gamma = \Psi_m \sum T_{RP}(\lambda)\eta(\lambda)\Delta(\lambda) \tag{13}$$

where Ψ_m is a constant, $\eta(\lambda)$ is the relative photopic luminous efficiency function, and $\Delta(\lambda)$ is the wavelength interval.

The WLED color properties also depend on the spectral power distributions, which depend on the relative radiant power of the phosphor-converted photons in both layers. Figure 7 plots the CRIs of two-layer and mixed one-layer WLEDs with various red phosphor concentrations at correlated color temperature (CCT) 7700 K and 8500 K. Theoretical calculation and ray-tracing simulation spectra agree well. The CRIs values are quite different between two phosphor configurations, although the amount of yellow and red phosphors are equal in all cases. The two- layer package, which supports longer-wavelength red phosphor than the single-layer one, yields about 5% higher CRI output. With the increment of red phosphor concentration, the CRI moves up to the same extent in both two-layer and mixed one-layer LEDs under CCT modes. This indicates that their scattering and illumination characteristics are the same; however, for two-layer LED packages the chromaticity of LED can be efficiently adjusted by the ratio of blue to yellow and red components since the yellow phosphor does not absorb the backscattering of red emission from the upper red phosphor layer. This can confirm that the emission energy loss is associated with the re-absorption process by different phosphor emission spectrum within the LED packages.

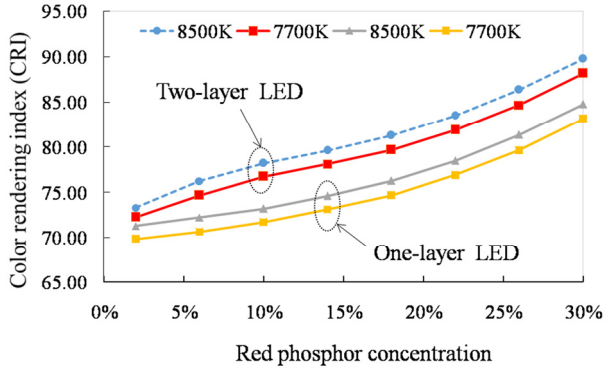

FIG. 7. CRI of two-layer and mixed one-layer LED with various red phosphor concentrations.

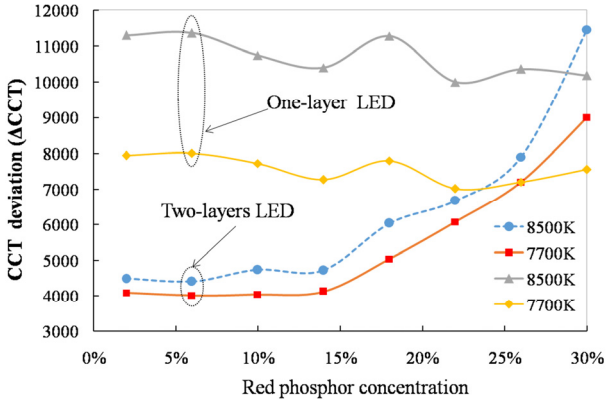

FIG. 8. CCT deviation of two-layer and mixed one-layer LED with various red phosphor concentrations.

One more improvement of the CRI is to overcome the derating of light sources at very low and very high CCTs below 3500 K and above 6500 K, respectively. The different CCT deviations should be required in various typical standards for WLED applications. The higher CCT deviation would lead to non-uniform white color at different angles because the light passes through the phosphor layer with higher concentration to be a smaller CCT deviation. As a result, the different lights could be mixed perfectly to form the uniform white light. That is the reason why CCT deviation in one-layer LED package decreases a little with the increment of α-$SrO{\cdot}3B_2O_3:Sm^{2+}$ concentration percentage in Fig. 8. Meanwhile, CCT deviation in two-layer LED package, where yellow phosphor layer concentration is fixed at 15% and α-$SrO{\cdot}3B_2O_3:Sm^{2+}$ concentration rises from 2% to 15%, changes insignificantly. However, with red phosphor concentration higher than 15%, CCT deviation tends to increase significantly due to scattering and backscattering in red phosphor layer with α-$SrO{\cdot}3B_2O_3:Sm^{2+}$ particles to be raised up as in Figs. 2(a) and 3. As a result, non-uniform WLED color is generated at different angles. These results are the different spectral power distribution of light from two different phosphor configurations such as Fig. 5.

IV. CONCLUSION

Remote phosphor multi-chip WLEDs with separating α-$SrO{\cdot}3B_2O_3:Sm^{2+}$ (red) and YAG:Ce (yellow) phosphor layers are studied under different α-$SrO{\cdot}3B_2O_3:Sm^{2+}$ concentration conditions. It is found that this new packaging method with red-emitting α-$SrO{\cdot}3B_2O_3:Sm^{2+}$ phosphor leads to at least more than 17% increasing in lumen compared to traditional mixed red and a yellow phosphor packaging at the same correlated color temperature. The effect of higher additional concentration α-$SrO{\cdot}3B_2O_3:Sm^{2+}$ of two-layer RP-WLEDs is also observed. This improvement in uniform color properties is due to increased scattering and back reflection of light inside the packages. The CRI of two-layer remote phosphor white LEDs is almost 5% higher than mixed phosphor white LEDs in α-$SrO{\cdot}3B_2O_3:Sm^{2+}$ concentrating regulation condition. The technology of two-layer remote phosphor multi-chip WLED package that employs α-$SrO{\cdot}3B_2O_3:Sm^{2+}$ phosphor can give high lumen and color rendering index and allowable uniform color range. These results offer a prospective practical solution for manufacturing two-layer remote phosphor WLEDs. In further works, the influence of α-$SrO{\cdot}3B_2O_3:Sm^{2+}$ phosphor features on the lighting performance of RP-WLEDs will be more developed.

REFERENCES

1. P.-C. Wang, Y.-K. Su, C.-L. Lin, and G.-S. Huang, "Improving Performance and Reducing Amount of Phosphor

Required in Packaging of White LEDs With TiO_2-Doped Silicone," IEEE Electron Device Lett. **35**(6), 657-659 (2014), doi: 10.1109/LED.2014.2318037.
2. M. Arik, C. Becker, S. Weaver, and J. Petroski, "Thermal management of LEDs: package to the system," Proc. SPIE **5187**, 64 (2004).
3. R. Mueller-Mach, G. O. Mueller, M. R. Krames, and T. Trottier, "High-power phosphor converted light-emitting diodes based on III-nitrides," IEEE J. Sel. Top. Quantum Electron. **8**(2), 339-345 (2002).
4. J. P. You, N. T. Tran, Y. C. Lin, Y. He, and F. G. Shi, "Phosphor-concentration-dependent characteristics of white LEDs under different current regulation modes," J. Electron. Mater. **38**(6), 761-766 (2009).
5. N. Narendran, Y. Gu, J. P. Freyssinier-Nova, and Y. Zhu, "Extracting phosphor-scattered photons to improve white LED efficiency," Phys. Status Solidi., A Appl. Mater. Sci. **202**(6), R60-R62 (2005).
6. H. Luo, J. K. Kim, E. F. Schubert, J. Cho, C. Sone, and Y. Park, "Analysis of high-power packages for phosphor based white-light-emitting diodes," Appl. Phys. Lett. **86**(24), 243505-243507 (2005).
7. J. K. Kim, H. Luo, E. F. Schubert, J. Cho, C. Sone, and Y. Park, "Strongly enhanced phosphor efficiency in GaInN white light-emitting diodes using remote phosphor configuration and diffuse reflector cup," Jpn. J. Appl. Phys. **44**(21), L649-L651 (2005).
8. K. K. Seong, T. W. Yoo, B.-S. Kim, S. M. Lee, Y. S. Lee, and L. S. Park. "White LED packaging with layered encapsulation of quantum dots and optical properties." J. Mol. Cryst. Liq. Cryst. **564**(1), 33-41 (2012), doi: 10.1080/15421406.2012.690655.
9. S. C. Allen and A. J. Steckl, "ELiXIR - Solid-state luminaire with enhanced light extraction by internal reflection," J. Disp. Technol. **3**(2), 155-159 (2007).
10. S. C. Allen and A. J. Steckl, "A nearly ideal phosphor-converted white light-emitted diode," J. Appl. Phys. **92**, 143309-143311 (2008).
11. H. Masui, S. Nakamura, and S. P. Denbaars, "Effects of phosphor application geometry on white light-emitting diodes," Jpn. J. Appl. Phys. **45**(34), L910-L912 (2006).
12. N. D. Q. Anh, M. F. Lai, H. Y. Ma, and H. Y. Lee, "Enhancing of correlated color temperature uniformity for multichip white light LEDs by adding SiO_2 to phosphor layer." J. Chin. Inst. Eng. **38**(3), (2015), doi: 10.1080/02533839.2014.981214.
13. R. Mueller-Mach, G. Mueller, M. R. Krames, H. A. Hoppe, F. Stadler, W. Schnick, T. Juestel, and P. Schmidt, "Highly efficient all-nitride phosphor-converted white light emitting diode," Phys. Status Solidi A **202**(9)**,** 1727-1732 (2005).
14. R. Hu, B. Cao, Y. Zou, Y. Zhu, and X. Luo, "Modeling the light extraction efficiency of Bi-layer phosphors in white LEDs," IEEE Photon. Technol. Lett. **25**(12), (2013).
15. C. H. Chiang, S. J. Gong, T. S. Zhan, and S. Y. Chu, "White light-emitting diodes with high color rendering index and tunable color temperature fabricated using separated phosphor layer structure." IEEE Electron Device Lett. (2016), doi: 10.1109/LED.2016.2576498.
16. Y. Zhu and N. Narendran, "Investigation of remote-phosphor white light-emitting diodes with multi-phosphor layers," Jpn. J. Appl. Phys. **49**(10R), 100203, 3pp (2010), doi: 10.1143/JJAP.49.100203.
17. W. M. Yen and M. J. Weber, *Inorganic phosphors: compositions, preparation and optical properties*, Washington, D. C. CRC Press, (2004).
18. T. H. Q. Minh, N. H. K. Nhan, and N. D. Q. Anh, "Red-emitting α-SrO·3B_2O_3:Sm^{2+}phosphor: An innovative application for increasing color quality and luminous flux of remote phosphor white LEDs," J. Chin. Inst. Eng. (2016).
19. P. Kubelka and F. Munk, "Ein beitrag zur optik der farbanstriche," Z. Tech. Phys. **12**, 593-601 (1931).
20. P. S. Mudgett and L. W. Richards, "Multiple scattering calculations for technology," Appl. Opt. **10**, 1485-1501 (1971).
21. B. J. Brinkworth, "Interpretation of the Kubelka - Munk coefficients in reflection theory," Appl. Opt. **1**, 1434-1435, (1972).
22. H. Reiss, *Radiative Transfer in Nontransparent Dispersed Media*, Springer, Berlin, (1988).
23. J. Zhong, M. Xie, Z. Ou, R. Zhang, M. Huang, and F. Zhao., "Mie theory simulation of the effect on light extraction by 2-D nanostructure fabrication," in *Proceedings Symposium on Photonics and Optoelectronics (SOPO), IEEE* (2011).
24. G. Wyszecki and W. S. Stiles, *Color science - concepts and methods, quantitative data and formulae*, Wiley, 2nd edition, p. 156, New York, (1982).
25. H. Chen and S. Y. (Ron) Hui, "Dynamic prediction of correlated color temperature and color rendering index of phosphor-coated white light-emitting diodes," IEEE Trans. Ind. Electron. **61**(2), (2014).